Available online at www.sciencedirect.com
SCIENCE DIRECT®
Journal of Computational Physics 214 (2006) 421–445
JOURNAL OF COMPUTATIONAL PHYSICS
www.elsevier.com/locate/jcp

Numerical methods for multiscale elliptic problems

Pingbing Ming [a,*], Xingye Yue [b]

[a] Institute of Computational Mathematics and Scientific/Engineering Computing, Academy of Mathematics and System Sciences, AMSS, Chinese Academy of Sciences, No. 55, Zhong-Guan-Cun East Road, Beijing 100080, China
[b] Department of Mathematics, Suzhou University, Suzhou 215006, China

Received 16 December 2003; received in revised form 20 August 2005; accepted 26 September 2005
Available online 9 November 2005

Abstract

We present an overview of the recent development on numerical methods for elliptic problems with multiscale coefficients. We carry out a thorough study of two representative techniques: the heterogeneous multiscale method (HMM) and the multiscale finite element method (MsFEM). For problems with scale separation (but without specific assumptions on the particular form of the coefficients), analytical and numerical results show that HMM gives comparable accuracy as MsFEM, with much less cost. For problems without scale separation, our numerical results suggest that HMM performs at least as well as MsFEM, in terms of accuracy and cost, even though in this case both methods may fail to converge. Since the cost of MsFEM is comparable to that of solving the full fine scale problem, one might expect that it does not need scale separation and still retains some accuracy. We show that this is not the case. Specifically, we give an example showing that if there exists an intermediate scale comparable to H, the size of the macroscale mesh, then MsFEM commits a finite error even with overlapping.

MSC: 65N30; 74Q05; 74Q15; 74Q20; 39A12

Keywords: Heterogeneous multiscale method; Multiscale finite element method; Scale separation

1. Introduction

In recent years the numerical computation of multiscale problems have emerged as an area of great promise. Among the most discussed examples is the elliptic problem with multiscale coefficients:

$$\begin{cases} -\operatorname{div}(a^\varepsilon(\boldsymbol{x})\nabla u^\varepsilon(\boldsymbol{x})) = f(\boldsymbol{x}) & \text{in } D, \\ u^\varepsilon(\boldsymbol{x}) = g(\boldsymbol{x}) & \text{on } \partial D, \end{cases} \tag{1.1}$$

where $\varepsilon \ll 1$ is a parameter that represents the ratio of the smallest and largest scales in the problem. This problem has attracted a great deal of attention because of its simplicity, its relevance to several important practical problems such as flow in porous media and mechanical properties of composite materials, and the

* Corresponding author. Tel.: +86 10 62626583; fax: +86 10 62542285.
E-mail addresses: mpb@lsec.cc.ac.cn (P. Ming), xyyue@suda.edu.cn (X. Yue).

0021-9991/$ - see front matter © 2005 Elsevier Inc. All rights reserved.
doi:10.1016/j.jcp.2005.09.024

extensive analytical work that has been done on it. Several different but related numerical techniques have been proposed, including wavelet homogenization techniques [17], multigrid numerical homogenization techniques [27,28,38,39], solving analytical or effective homogenized equations [10,16,15,41], finite element methods with multiscale test and trial functions [4,6], the multiscale finite element method (MsFEM) [31,32,24], finite element method based on the *Residual-Free Bubble* method (or the variational multiscale method, Discontinuous enrichment method) [12,33,29,43,26], and the heterogeneous multiscale method (HMM) [19–22]. The purpose of the present paper is to give an overview of these methodologies as well as a thorough study of two representative techniques: MsFEM and HMM.

Before we discuss the more recent techniques, let us say a few words about some classical multiscale techniques that have been very successful for elliptic problems, e.g., the multi-grid method [11,2] and the fast multipole method [30]. Multi-grid method achieves optimal efficiency by relaxing the errors at different scales on different grids. It gives an accurate approximation to the detailed solutions of the fine scale problem (1.1). In contrast, with the exception of MsFEM, the more recent activities center around designing multiscale methods with sublinear complexity [21], i.e., the computational cost scales sublinearly with the cost of solving the fine scale problem as $\varepsilon \to 0$. It is important to realize that our perspective has to be modified somewhat for this purpose. First, we have to ask for less about the details of the solutions, since in many cases this would require us to solve the full fine scale problem and this already defeats our purpose. Secondly, we have to explore special features of the problem, such as self-similarity, periodicity and scale separation. This means that the method cannot be fully general but rather relies on special assumptions on the coefficients. Indeed if a^ε does not have any special features, (1.1) is just as hard as a general elliptic problem:

$$\begin{cases} -\operatorname{div}(a(\boldsymbol{x})\nabla u(\boldsymbol{x})) = f(\boldsymbol{x}) & \text{in } D, \\ u(\boldsymbol{x}) = g(\boldsymbol{x}) & \text{on } \partial D, \end{cases}$$

and we cannot hope for a method with sublinear cost. On the other hand, it is undesirable for the numerical methods to have a too small range of applicability. Therefore a balance has to be reached between specificity and generality. One common feature found in many practical problems is separation of scales. Indeed it has been the designing principle of many modern multiscale methods such as HMM to be able to take full advantage of the possible scale separation in the problem, while in the absence of scale separation, the method is similar to the fine scale solvers. We must emphasize that scale separation does not mean the coefficient a^ε takes the form $a^\varepsilon(\boldsymbol{x}) = a(\boldsymbol{x}/\varepsilon)$ with $a(\cdot)$ a periodic function and ε a small parameter. Though this is indeed an important case. There are some other cases of scale separation, for example, the coefficient a^ε is a locally stationary random fields.

One exception is MsFEM. For problems of the type (1.1), MsFEM incurs a cost that is comparable to that of a fine scale solver, even for problems with scale separation. For this reason, one might expect that MsFEM might still retain some accuracy even for problems without scale separation, as in the case of fine scale solvers. We will show that this is not the case. Specifically, we will give explicit examples showing that MsFEM converges to the wrong solution if there is an intermediate scale which is comparable to the size of the macroscale mesh.

There are many important problems without separation of scales. In the absence of a better understanding at the present time the options for such problems seem to be either the full fine scale solvers or resorting to ad hoc procedures such as turbulence models. Other special features have to be identified in order to construct sublinear algorithms that do not resort to uncontrolled approximations.

This paper is organized as follows. In the following section, we will give an overview of the different multiscale methods. Sections 3 and 4 are devoted to a thorough study of HMM and MsFEM. We pick these two methods since they represent two somewhat opposite philosophies. Section 3 is devoted to problems with scale separation. This is the case when both methods have been thoroughly analyzed. Here, we compare the cost and accuracy of HMM and MsFEM for several classes of problems. We will show that MsFEM incurs an $\mathcal{O}(1)$ error if the specific details of the fine scale properties are not explicitly used. In Section 4, we consider problems without scale separation. In this case both methods may fail to converge but we show that in terms of numbers, the quality of the HMM result is at least comparable to that of MsFEM. Finally, we draw some conclusions in Section 5.

2. An overview of multiscale methods

To present the methods, we consider the typical multiscale problem

$$\begin{cases} -\mathrm{div}(a^\varepsilon(\boldsymbol{x})\nabla u^\varepsilon(\boldsymbol{x})) = f(\boldsymbol{x}) & \text{in } D, \\ u^\varepsilon(\boldsymbol{x}) = 0 & \text{on } \partial D, \end{cases} \tag{2.1}$$

where $a^\varepsilon(\boldsymbol{x}) = (a^\varepsilon_{ij}(\boldsymbol{x}))$ is assumed to be a symmetric matrix satisfying

$$\lambda|\xi|^2 \leqslant \sum_{i,j=1}^{2} a^\varepsilon_{ij}\xi_i\xi_j \leqslant \Lambda|\xi|^2 \quad \forall \xi \in \mathbb{R}^2,$$

with $0<\lambda \leqslant \Lambda$.

We will use standard notations for Sobolev spaces $W^{k,p}(D)$ [1] for $k>0$ and $p>1$, which are denoted by $H^k(D)$, while $p=2$.

2.1. General methodologies

2.1.1. Generalized finite element method

Generalized finite element method [7,6] is a finite element method on a macroscopic mesh with modified basis functions that are obtained by solving (1.1) with $f=0$ and nodal boundary conditions. This method is a perfect strategy for one dimensional problems. It was extended to high dimensions in [31]. Other methods for modifying the basis functions are found in [12,33].

2.1.2. Wavelet homogenization

The main idea is to numerically derive effective operators at the macroscale by successively eliminating the small scales. The most natural framework for carrying this out is to represent the numerical solutions in wavelet basis [17]. Even though after eliminating the smaller scales, the effective operator becomes dense, Engquist and Runborg [25] have shown that they can be very well approximated by sparse operators.

2.1.3. Model refinement

One of the most important issues in solving problems of the type (1.1) is to recover the details of ∇u^ε since they contain information of great practical interest, such as the stress distribution in a composite material or velocity field in a porous medium. Oden and Vemaganti [41] proposed the idea of local model refinement for this purpose. After the homogenized equation is solved, the original fine scale problem is solved locally around places where derivative information is required, with the homogenized solution as the Dirichlet boundary condition. Denote by Ω the domain in which the microscale information of u^ε is needed. Consider the following auxiliary problem:

$$\begin{cases} -\mathrm{div}(a^\varepsilon(\boldsymbol{x})\nabla \overline{u}^\varepsilon(\boldsymbol{x})) = f(\boldsymbol{x}), & \boldsymbol{x} \in \Omega_\eta, \\ \overline{u}^\varepsilon(\boldsymbol{x}) = U_H(\boldsymbol{x}), & \boldsymbol{x} \in \partial\Omega_\eta, \end{cases} \tag{2.2}$$

where Ω_η satisfies $\Omega \subset \Omega_\eta \subset D$ and $\mathrm{dist}(\partial\Omega,\partial\Omega_\eta) = \eta$. We then have

$$\left(\frac{1}{|\Omega|}\int_\Omega |\nabla(u^\varepsilon - \overline{u}^\varepsilon)|^2 \,\mathrm{d}\boldsymbol{x}\right)^{1/2} \leqslant \frac{C}{\eta}\left(\|U_0 - U_H\|_{L^\infty(\Omega_\eta)} + \|u^\varepsilon - U_0\|_{L^\infty(\Omega_\eta)}\right). \tag{2.3}$$

Here U_H and U_0 are, respectively, the numerical and analytical solutions to the homogenized problem.

2.1.4. Heterogeneous multiscale method

There are two main components in the heterogeneous multiscale method: An overall macroscopic scheme for the macro-scale variables on a macroscale grid and estimating the missing macroscopic data from the microscopic model. For (1.1), the macroscopic solver can be chosen simply as the standard piecewise linear finite element method over a macroscopic triangulation $\mathcal{T}_H$ of mesh size H. The data that need to be estimated is the stiffness matrix. This is equivalent to evaluating the effective quadratic form $A(V,V)$

for $V \in X_H$, where X_H is the macroscopic finite element space. If we had an explicit expression for $A(V,V)$, such as

$$A(V,V) = \int_D \sum_{i,j=1}^{2} A_{ij}(\boldsymbol{x}) \frac{\partial V}{\partial x_i} \frac{\partial V}{\partial x_j} \, \mathrm{d}\boldsymbol{x}, \tag{2.4}$$

we can then evaluate the integral by numerical quadrature. In the absence of an explicit representation such as (2.4), we need to estimate the value of the integrand in (2.4) at quadrature points. This is done as follows.

Let $\boldsymbol{x}_K$ be the barycenter of the element $K \in \mathscr{T}_H$, and left $I_\delta = \boldsymbol{x}_K + \delta I$, where $I = [0,1]^2$ (see the let one in Fig. 2). δ is chosen such that a^ε restricted to I_δ gives an accurate enough representation of the local variations of a^ε. For $V \in X_H$, let $\mathscr{R}(V)$ be the solution of

$$\operatorname{div}(a^\varepsilon(\boldsymbol{x}) \nabla \mathscr{R}(V)) = 0, \qquad \boldsymbol{x} \in I_\delta, \tag{2.5}$$

with $\mathscr{R}(V) = V$ on the boundary.

We then approximate the integrand of (2.4) at $\boldsymbol{x}_K$ by

$$\sum_{i,j=1}^{2} A_{ij}(\boldsymbol{x}_K) \frac{\partial V}{\partial x_i} \frac{\partial V}{\partial x_j} \approx \frac{1}{|I_\delta|} \int_{I_\delta} \sum_{i,j=1}^{2} a^\varepsilon_{ij}(\boldsymbol{x}) \frac{\partial}{\partial x_i} \mathscr{R}(V) \frac{\partial}{\partial x_j} \mathscr{R}(V) \, \mathrm{d}\boldsymbol{x}. \tag{2.6}$$

The approximating bilinear form A_H is defined as

$$A_H(V,W) := \sum_{K \in \mathscr{T}_H} \frac{|K|}{|I_\delta|} \int_{I_\delta} \sum_{i,j=1}^{2} a^\varepsilon_{ij}(\boldsymbol{x}) \frac{\partial}{\partial x_i} \mathscr{R}(V) \frac{\partial}{\partial x_j} \mathscr{R}(W) \, \mathrm{d}\boldsymbol{x},$$

for any V, $W \in X_H$. The HMM solution $U_H \in X_H$ is defined by

$$A_H(U_H, V) = (f, V) \quad \text{for all} \quad V \in X_H. \tag{2.7}$$

HMM can be naturally extended to higher order by using higher order finite elements as the macroscopic solver (see [22] and also Fig. 1 for a schematic showcase for the quadratic element as a macroscale solver). In this case, a cell problem has to be solved at each quadrature point, and the higher-order numerical quadrature scheme has to be employed to approximate the bilinear form. HMM can also be extended to the case when the isoparametric finite elements are exploited as the macroscopic solver.

So far the formulation of HMM is completely general. The main point, however, is that HMM offers substantially savings of cost (compared to solve the full fine scale problems) for problems with scale separation. This is done by appropriately choosing δ. If the problem happens to be locally periodic, we may choose I_δ to be the local period. However, it is important to emphasize that it is not necessary for the coefficient $a^\varepsilon(\boldsymbol{x})$ to have the form $a(\boldsymbol{x},\boldsymbol{x}/\varepsilon)$ in order to have such savings, so long as there is scale separation. Without scale separation or any other special features of the problem, we simply employ a fine scale solver instead of HMM.

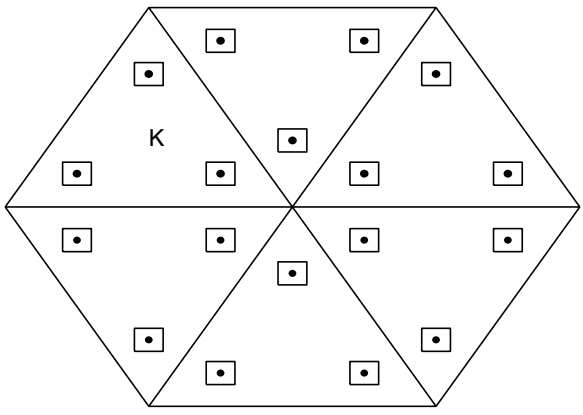

Fig. 1. Illustration of HMM for solving (1.1). The dots are the quadrature points. The little squares are the microcell I_δ.

In many cases, we would like to have accurate information on ∇u^ε. From U_H, one can construct an approximation $\overline{u}^\varepsilon$ to u^ε. A general strategy for constructing $\overline{u}^\varepsilon$ is to use the method of local corrections, as done by Oden and Vemaganti [41] (see also (2.2) and (2.3)), we refer to [22, Theorem 1.4] for the analysis of this strategy. For the special case of periodic homogenization problems, with $\delta = \varepsilon$, one may simply define on each element K,

$$\overline{u}^\varepsilon = U_H + (\mathscr{R}(U_H) - U_H)_p,$$

where $(f)_p$ means the periodic extension of f outside I_δ.

Even though the method is quite general, the analysis of HMM has so far only been carried out for the case when $a^\varepsilon(\boldsymbol{x}) = a(\boldsymbol{x},\boldsymbol{x}/\varepsilon)$. We firstly discuss the case when $a(\boldsymbol{x},\boldsymbol{y})$ is periodic in $\boldsymbol{y}$, say with period $I = [0,1]^2$.

Theorem 2.1 [22, Theorems 1.1 and 1.2]. *Let u^ε, U_0 and U_H be the solution of (1.1), the homogenized equation and (2.7), respectively. If $a(x,y)$ is periodic in y with period I, then there exists a constant C such that*

$$\|U_0 - U_H\|_{H^1(D)} \leqslant C(H + v_0(\varepsilon,\delta)). \tag{2.8}$$

$$\|U_0 - U_H\|_{L^2(D)} \leqslant C(H^2 + v_0(\varepsilon,\delta)). \tag{2.9}$$

$$\|U_0 - U_H\|_{L^\infty(D)} \leqslant C(H^2 + v_0(\varepsilon,\delta))|\ln H| \tag{2.10}$$

Let $\overline{u}^\varepsilon$ be the reconstructed microstructure as above, we have

$$\left(\sum_{K\in\mathscr{T}_H} \|\nabla(u^\varepsilon - \overline{u}^\varepsilon)\|^2_{L^2(K)}\right)^{1/2} \leqslant C\left(\sqrt{\varepsilon} + H + v_0(\varepsilon,\delta)\right), \tag{2.11}$$

In general,

$$v_0(\varepsilon,\delta) \leqslant C\left(\frac{\varepsilon}{\delta} + \delta\right).$$

But if $\delta = \mathbb{N}\varepsilon$ and $\mathbb{N}$ is an integer, then

$$v_0(\varepsilon,\delta) \leqslant C\delta.$$

In view of (2.9) and (2.10) and the classic estimates for u^ε [5,9,49]:

$$\|u^\varepsilon - U_0\|_{L^2(D)} \leqslant C\varepsilon, \qquad \|u^\varepsilon - U_0\|_{L^\infty(D)} \leqslant C\varepsilon,$$

an application of the triangle inequality gives

$$\|u^\varepsilon - U_H\|_{L^2(D)} \leqslant C(\varepsilon + H^2 + v_0(\varepsilon,\delta)). \tag{2.12}$$

$$\|u^\varepsilon - U_H\|_{L^\infty(D)} \leqslant C(\varepsilon + H^2 + v_0(\varepsilon,\delta))|\ln H|. \tag{2.13}$$

Many practical problems are better modelled by an a^ε which is a locally stationary random field. We refer to [22] for the precise setting. In this case, we have:

Theorem 2.2 [22, Theorem 1.2]. *For the case when $a(\boldsymbol{x}, \boldsymbol{y})$ is stationary random field, under the conditions of* [22, Theorem 1.1], *we have*

$$\mathbb{E}\|U_0 - U_H\|_{H^1(D)} \leqslant C(H + v_0(\varepsilon,\delta)),$$

where

$$v_0(\varepsilon,\delta) \leqslant \begin{cases} C(\kappa)\left(\frac{\varepsilon}{\delta}\right)^\kappa & d = 3, \\ \text{remains open} & d = 2, \\ C\left(\frac{\varepsilon}{\delta}\right)^{1/2} & d = 1, \end{cases}$$

with

$$\kappa = \frac{6 - 12\gamma}{25 - 8\gamma} \qquad 0 < \gamma < \frac{1}{2}.$$

The conditions in [22, Theorem 1.2] are mainly strong mixing, uniform ellipticity and some regularity on $a(\boldsymbol{x},\boldsymbol{y})$.

2.1.5. MsFEM

We discuss the over-sampling MsFEM[31,24] which reduces the effect of the boundary layers occurring at the inter-element boundaries. MsFEM is an extension of an old idea of Babuska [7], which incorporates the fine scale information into the basis functions by solving the original fine scale differential equations on each element with proper boundary conditions.

For any $K \in \mathscr{T}_H$ with nodes $\{x_i^K\}_{i=1}^3$, let H_K denote the size of K, $P_1(K)$ the set of linear polynomials defined in K, and $\{\varphi_i^K\}_{i=1}^3$ the basis of $P_1(K)$ satisfying $\varphi_i^K(x_j^K) = \delta_{ij}, i,j = 1,2,3$. For any $K \in \mathscr{T}_H$, we denote by $S = S(K)$ (see Fig. 2) a macro-element which contains K and satisfies the following conditions: $H_S \leqslant C_1 H_K$ and $\mathrm{dist}(\partial K, \partial S) \geqslant \delta_0 H_K$ for some positive constants C_1, δ_0 independent of H.

Let $MS(S)$ be the multiscale finite element space spanned by $\psi_i^S, i = 1,2,3$, with $\psi_i^S \in H^1(S)$ being the solution of the problem

$$-\mathrm{div}\left(a^\varepsilon(x)\nabla\psi_i^S\right) = 0 \quad \text{in } S, \quad \psi_i^S|_{\partial S} = \varphi_i^S. \tag{2.14}$$

Here $\{\varphi_i^S\}_{i=1}^3$ is the nodal basis of $P_1(S)$ such that $\varphi_i^S(x_j^S) = \delta_{ij}$, $i,j = 1,2,3$. The over-sampling multiscale finite element base functions over K are defined by

$$\bar{\psi}_i^K = c_{ij}^K \psi_j^S|_K \quad \text{in } K$$

with the constants c_{ij}^K is chosen that

$$\varphi_i^K = c_{ij}^K \varphi_j^S|_K \quad \text{in } K.$$

The existence of the constants c_{ij}^K is guaranteed because $\{\varphi_j^S\}_{j=1}^3$ also forms the basis of $P_1(K)$.

Let $\mathscr{M}(K) = \mathrm{span}\{\bar{\psi}_i^K\}_{i=1}^3$ and $\Pi_K : \mathscr{M}(K) \to P_1(K)$ the projection

$$\Pi_K \psi = c_i \varphi_i^K \quad \text{if } \psi = c_i \bar{\psi}_i^K \in \mathscr{M}(K).$$

Let $\overline{V}_H$ be the finite element space

$$\overline{V}_H = \{\psi_H \mid \psi_H|_K \in \mathscr{M}(K),\ \forall K \in \mathscr{T}_H\},$$

and define $\Pi_H : \overline{V}_H \to \Pi_{K\in\mathscr{T}_H} P_1(K)$ through the relation $\Pi_H \psi_H|_K = \Pi_K \psi_H$ for any $K \in \mathscr{T}_H$, $\psi_H \in \overline{V}_H$. The over-sampling multiscale finite element space is then defined as

$$V_H = \{\psi_H \in \overline{V}_H \mid \Pi_H \psi_H \in X_H \subset H_0^1(D)\}.$$

The over-sampling MsFEM is: Find $U_H \in V_H$ such that

$$\sum_{K\in\mathscr{T}_H} \int_K a^\varepsilon(\boldsymbol{x})\nabla U_H \nabla V \,\mathrm{d}\boldsymbol{x} = (f, V) \quad \text{for all} \quad V \in V_H. \tag{2.15}$$

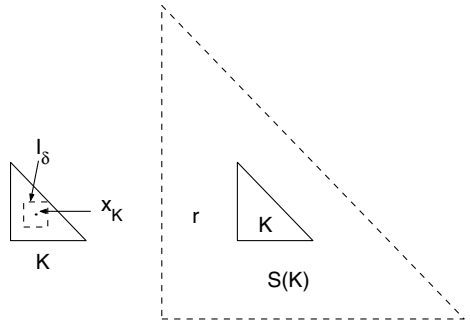

Fig. 2. Computational cell used for solving fine scale problem in HMM and MsFEM. The element K is depicted in solid line. The computational cell I_δ for HMM and $S(K)$ for MsFEM are depicted in dashed line.

The analysis of MsFEM has only been carried out for the case when $a^\varepsilon(\boldsymbol{x}) = a(\boldsymbol{x}/\varepsilon)$ and $a(\boldsymbol{y})$ is periodic in $\boldsymbol{y}$, in this case, we have

Theorem 2.3. [32,24] *Let u^ε and U_H be the solutions of (2.1) and (2.15), respectively. If $a(y)$ is periodic with period I, then there exists a constant C which is independent of ε, δ and H such that*

$$\left(\sum_{K\in\mathscr{T}_H} \|\nabla(u^\varepsilon - U_H)\|^2_{L^2(K)}\right)^{1/2} \leqslant C\left(\sqrt{\varepsilon} + H + \frac{\varepsilon}{H}\right), \tag{2.16}$$

and

$$\|u^\varepsilon - U_H\|_{L^2(D)} \leqslant C\left(H^2 + \frac{\varepsilon}{H}\right). \tag{2.17}$$

The above error bounds may be extended to the locally periodic coefficients, i.e., $a^\varepsilon(\boldsymbol{x}) = a(\boldsymbol{x},\boldsymbol{x}/\varepsilon)$ with $a(\cdot,\boldsymbol{y})$ is periodic in $\boldsymbol{y}$ by combining the techniques in [13] and [32,24,48]. However, the accuracy in L^2 norm may deteriorate if the algorithm is not adopted to the new feature of the coefficients.

If $a^\varepsilon(\boldsymbol{x}) = a(\boldsymbol{x}/\varepsilon)$ with $a(\boldsymbol{y})$ is periodic, then (2.12) and (2.13) can be improved to

$$\|u^\varepsilon - U_H\|_{L^2(D)} \leqslant C\left(H^2 + \frac{\varepsilon}{\delta}\right),$$
$$\|u^\varepsilon - U_H\|_{L^\infty(D)} \leqslant C\left(H^2 + \frac{\varepsilon}{\delta}\right)|\ln H|.$$

In view of the above two estimates (2.11) and Theorem 2.3, we may conclude that the accuracy of HMM and MsFEM is comparable in this special case since we always assume that δ is commensurable with H. Moreover, once we know the exact period of a^ε, we only need to solve the cell problem over I_ε, in this case, the consistency error term ε/δ vanishes, HMM get better results.

2.2. Special techniques for the periodic homogenization problem

Next, we discuss methods that are more specific. Such methods rely on a specific form of the coefficient $a^\varepsilon(\boldsymbol{x}) = a(\boldsymbol{x},\boldsymbol{x}/\varepsilon)$, where the function $a(\boldsymbol{x},\boldsymbol{y})$ is periodic in $\boldsymbol{y}$ with some period, say I.

2.2.1. Solving homogenized equations

Since there exists a very well-developed homogenization theory, one may use these theory for numerical purposes. This is done for example in [10,4,16,15] . The leading order term in u^ε is obtained by solving the homogenized equation:

$$\begin{cases} -\mathrm{div}(A(\boldsymbol{x})\nabla U(\boldsymbol{x})) = f(\boldsymbol{x}) & \text{in } D, \\ U(\boldsymbol{x}) = g(\boldsymbol{x}) & \text{on } \partial D. \end{cases} \tag{2.18}$$

To obtain finite ε correction and to recover the microstructural behavior of u^ε, one needs to solve further the corrector problem: find $u_1(\boldsymbol{x},\boldsymbol{x}/\varepsilon)$ such that

$$\begin{cases} -\mathrm{div}\left(a^\varepsilon(\boldsymbol{x})\nabla u_1\left(\boldsymbol{x},\frac{\boldsymbol{x}}{\varepsilon}\right)\right) = \mathrm{div}(a^\varepsilon(\boldsymbol{x})\nabla U_0(\boldsymbol{x})) & \text{in } D, \\ u_1(\boldsymbol{x},\boldsymbol{y}) & \text{is periodic in } \boldsymbol{y}. \end{cases}$$

A subtle issue in this approach is the presence of boundary layers [8]:

$$\|u^\varepsilon(\boldsymbol{x}) - \left(U_0(\boldsymbol{x}) + u_1\left(\boldsymbol{x},\frac{\boldsymbol{x}}{\varepsilon}\right)\right)\|_{H^1(D)} \leqslant C\sqrt{\varepsilon}.$$

2.2.2. Two-scale finite element methods

The main idea is to use multiscale test and trial functions of the form $\varphi(\boldsymbol{x},\boldsymbol{x}/\varepsilon)$ to probe simultaneously the macro and microscale behavior of the solution u^ε. The two-scale finite element space X_H is the traces of the two-scale spaces $\mathscr{S}^p(\mathscr{T}_H;\mathscr{S}^\mu_{\mathrm{per}}(\mathscr{T}_h))$,

$$X_H = \mathscr{R}^\varepsilon \mathscr{S}^p(\mathscr{T}_H; \mathscr{S}^\mu_{\text{per}}(\mathscr{T}_h)) \qquad \text{with} \qquad (\mathscr{R}^\varepsilon V)(x) = V(x,y)_{|_{y=\frac{x}{\varepsilon}}}.$$

Here the macroscopic finite element space $\mathscr{S}^p$ consists of piecewise polynomials of degree p over $\mathscr{T}_H$; and the finite element space over the cell εI, say $\mathscr{S}^\mu_{\text{per}}$, which consists of periodic piecewise polynomials of degree μ over the microscopic mesh $\mathscr{T}_h$. This idea has been used in the analytical work of Allaire [3], E [18] and Nguetseng [40], among others. The work of Schwab et al. [36,44,45] develop this into a numerical tool. The following result on the accuracy of this method is proved in [37]. Denote by u^ε_H the two-scale finite element solution. If H is an integer multiple of ε, then

$$\|u^\varepsilon - u^\varepsilon_H\|_{H^1(D)} \leqslant C_1(k) H^{\min(p,k)} \Phi_n(p,k) \|f\|_{H^k(D)} + C_2(s) h^{\min(\mu,s)} \Phi_n(\mu,s) \|f\|_{H^{\mu+s}(D)}. \tag{2.19}$$

Here $\Phi_n(p,k) \leqslant Cp^{-(k-n+1)}$ and $\Phi_n(\mu,s) \leqslant C\mu^{-(s-n+1)}$.

3. Problems with scale separation

3.1. Computational cost

To compare the cost we make the assumption that the total cost is proportional to the total degrees of the freedom used in the algorithm. This is reasonable since we typically use multi-grid method as the fine scale solver. Given parameters ε, H and δ, assuming that M points per wavelength (which is $\mathscr{O}(\varepsilon)$) are used, then the total cost for the full fine scale solver is

$$\text{COST(fine scale solver)} = M^d \varepsilon^{-d}.$$

Assuming that the size of the overlap in MsFEM is r, then the total cost for MsFEM is

$$\text{COST(MsFEM)} = (1+3r)^d M^d \varepsilon^{-d}.$$

The ratio between the two is

$$\frac{\text{COST(fine scale solver)}}{\text{COST(MsFEM)}} = \frac{1}{(1+3r/H)^d} < 1,$$

i.e., MsFEM is in general more expensive than the full fine scale solver.

The cost for HMM is:

$$\text{COST(HMM)} = M^d H^{-d} \left(\frac{\delta}{\varepsilon}\right)^d.$$

Hence the ratio between the cost of HMM and the cost of MsFEM is

$$\frac{\text{COST(HMM)}}{\text{COST(MsFEM)}} = \left(\frac{\delta}{H}\right)^d \frac{1}{(1+3r/H)^d}.$$

The ratio between the cost of HMM and the cost of the direct fine scale solver is

$$\frac{\text{COST(HMM)}}{\textit{COST}\text{(fine scale solver)}} = \left(\frac{\delta}{H}\right)^d.$$

As long as we can take $\delta < H$, HMM incurs a smaller cost than the full fine scale solver. As long as we can take $\delta < H + 3r$, HMM incurs a smaller cost than MsFEM.

The parameters δ and H are determined by the tolerance factor, denoted by TOL. For MsFEM, the accuracy cannot be better than $\sqrt{\varepsilon}$ (see the error estimates in Theorem 2.3), so to make a meaningful comparison, we have to take

$$\text{TOL} > \mathscr{O}\left(\sqrt{\varepsilon}\right).$$

HMM may incur an additional cost in order to recover locally the fine scale information. This is problem-dependent.

The above discussion is for general problems with scale separation. For the special case of periodic homogenization problems, we can take $\delta = \varepsilon$ for HMM, and modify MsFEM so that the solutions to the corrector problem can be used in constructing the basis function. In this case, the cost of both methods are comparable.

Some problems require solving (1.1) repeatedly with different right-hand side. In this case the macroscale stiffness matrix can be computed for once and used repeatedly. Both HMM and MsFEM can take advantage of this fact.

Compared with the full fine scale solutions, both HMM and MsFEM have the advantage that they are easily parallelized. It has been suggested that MsFEM saves in memory compared with direct fine scale solvers. This is only true if the microscale information is not required, or if it is recovered through a post-processing step as discussed for HMM. Otherwise the complete set of basis functions in MsFEM have to be stored in order to retrieve such information, leaving us with no savings in memory.

3.2. Numerical examples for two-scale problem

We will start with an example of the simplest two-scale problem, the periodic homogenization problem.

$$\begin{cases} -\operatorname{div}\left(a\left(\boldsymbol{x}, \frac{\boldsymbol{x}}{\varepsilon}\right)\nabla u^{\varepsilon}(\boldsymbol{x})\right) = f & \text{in } D, \\ u^{\varepsilon}(\boldsymbol{x}) = 0 & \text{on } \partial D, \end{cases} \tag{3.1}$$

where $f = 10$, and the coefficients $a(\boldsymbol{x},\boldsymbol{x}/\varepsilon)$ is defined as

$$a\left(\boldsymbol{x}, \frac{\boldsymbol{x}}{\varepsilon}\right) = \frac{1.5 + \sin(2\pi x/\varepsilon)}{1.5 + \sin(2\pi y/\varepsilon)} + \frac{1.5 + \sin(2\pi y/\varepsilon)}{1.5 + \cos(2\pi x/\varepsilon)} + \sin(4x^2y^2) + 1 \tag{3.2}$$

with $\boldsymbol{x} = (x,y)$.

The domain D is a unit square $(0,1)^2$. We first triangulate D into $NX \times NX$ small squares and then divide each square into two sub-triangles along its diagonal with positive slope. As a starting point, we test the accuracy of HMM, in particular, we consider the influence of microcell size over the accuracy. The results for the relative errors

$$\frac{\left(\sum_{K\in\mathscr{T}_H} \|u^{\varepsilon} - \overline{u}^{\varepsilon}\|^2_{H^1(K)}\right)^{1/2}}{\|u^{\varepsilon}\|_{H^1}}, \quad \frac{\|u^{\varepsilon} - U_H\|_{L^2}}{\|u^{\varepsilon}\|_{L^2}} \quad \text{and} \quad \frac{\|u^{\varepsilon} - U_H\|_{L^\infty}}{\|u^{\varepsilon}\|_{L^\infty}}$$

are shown in Table 1, and plotted in Fig. 3. The exact solutions u^{ε} are obtained by applying the Richardson extrapolation to the solutions by solving the problem with linear finite element on 1024×1024 and 2048×2048 meshes.

3.2.1. Accuracy of HMM for two-scale problem

We first fix the microcell size as $\delta = 1/32$, which is not an integer multiple of $\varepsilon = 1/79$.

Notice that the error in H^1 norm is consistent with the previous theoretic result, e.g. (2.11). However, in L^2 and L^∞ norms, the error increase at the finest mesh $H = 1/64$, instead of decrease as predicted by the error bounds (2.12) and (2.13). This scenario is not yet fully understood. But it should be due to the fact that in this case, the microcell is larger than the element, and some spurious information is sampled and polluted

Table 1
HMM for Problem 3.1 with coefficient (3.2), $\varepsilon = 1/79$ and microcell size $\delta = 1/32$ is fixed

NX	HMM		
	H^1 error	L^2 error	L^∞ error
8	0.41e + 0	0.17e − 1	0.19e − 1
16	0.27e + 0	0.12e − 1	0.13e − 1
32	0.73e − 1	0.64e − 2	0.71e − 2
64	0.34e − 1	0.87e − 2	0.19e − 1

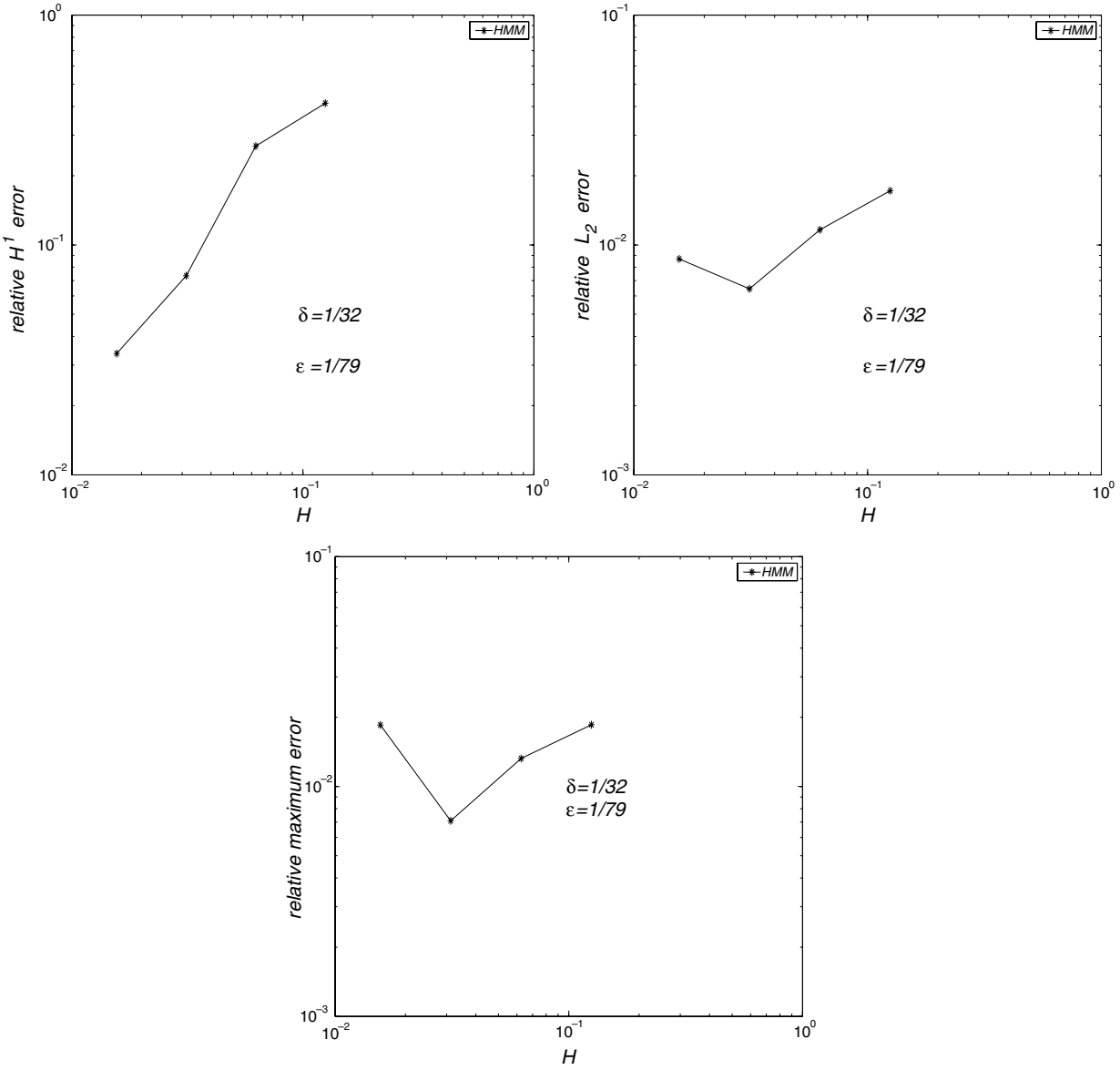

Fig. 3. Relative error in H^1, L^2 and L^∞ norms of HMM for Problem 3.1 with coefficients (3.2), where $\varepsilon = 1/79$.

the HMM solution. This is hidden in the term $\mathcal{O}(\delta)$, which obviously has more chance to dominant the error in L^2 and L^∞ norms than that in H^1 norm.

Next we fix the mesh size as $H = 1/32$, and change the microcell size δ.

The results in Tables 1, 2 and Figs. 3 and 4 fit quite well with the theoretic results. Note that the error increase while the microcell is larger than the element.

3.2.2. Comparison of HMM and MsFEM for two-scale problem

In the following examples, we compare the convergence behavior for HMM and MsFEM. Firstly, we consider the case when δ is not an integer multiply of ε in HMM. We include the results for $\delta = H$. The size of the overlap for MsFEM is taken as $r = \varepsilon$ (see Fig. 2). The results can be found in Table 3 and Fig. 5.

Secondly, we turn to a special case when $I_\delta = I_\varepsilon$ for HMM. The size of overlap for MsFEM is still $r = \varepsilon$. In this case, MsFEM can be modified to explicitly take into account the periodic structure of the original

Table 2
HMM for Problem 3.1 with coefficient (3.2), $\varepsilon = 1/79$ and $H = 1/32$ is fixed

$1/\delta$	HMM		
	H^1 error	L^2 error	L^∞ error
16	0.60e − 1	0.85e − 2	0.13e − 1
32	0.73e − 1	0.64e − 2	0.71e − 2
64	0.19e + 0	0.69e − 2	0.75e − 1

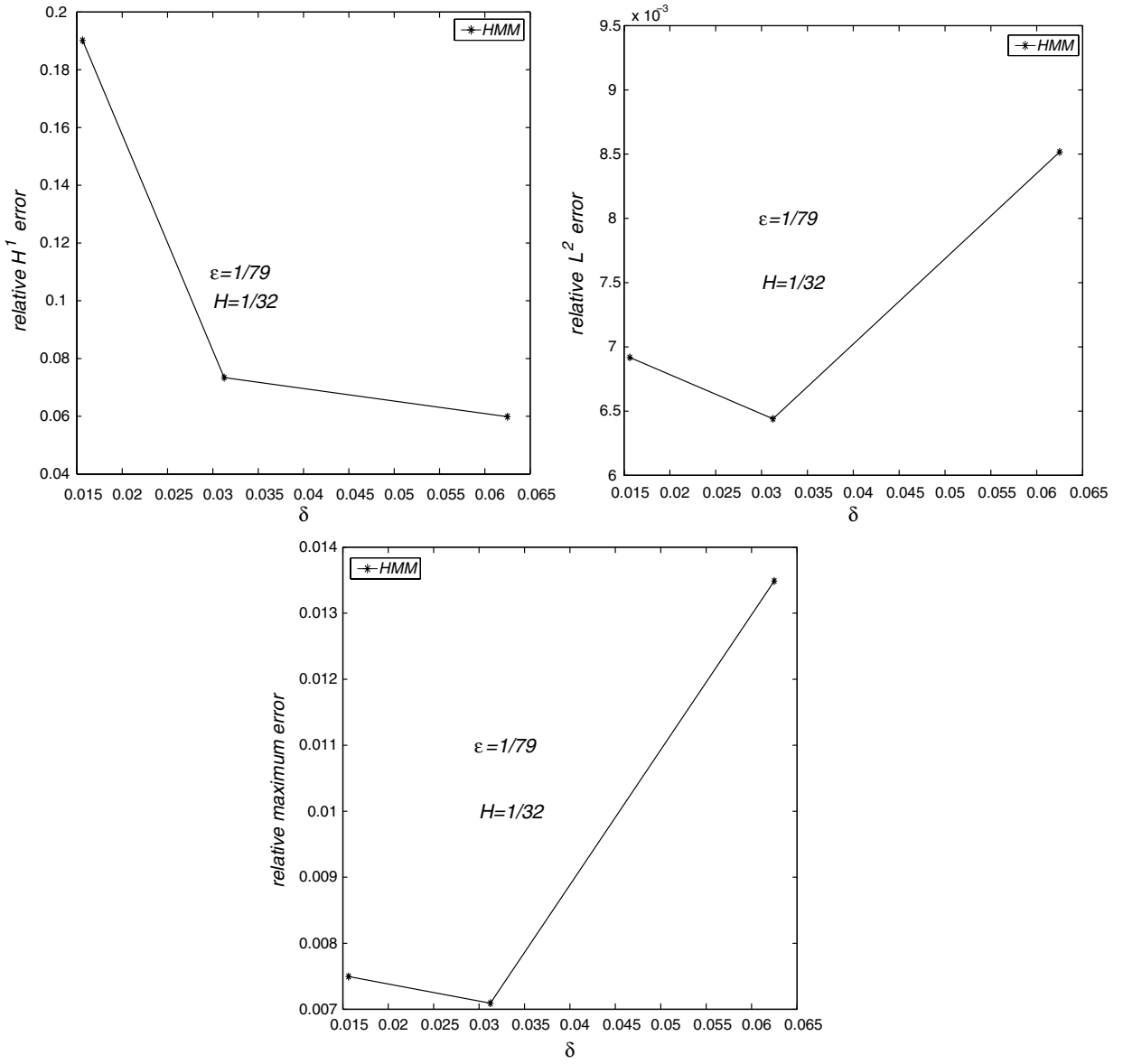

Fig. 4. Relative error in H^1, L^2 and L^∞ norms of HMM for Problem 3.1 with coefficients (3.2), where $\varepsilon = 1/79$ and $H = 1/32$ is fixed.

problem [23] by using the solutions of the cell problem as the basis function. But we will not consider this modification here, since it is too specifical and this case is not the main focus. The numerics are included in Table 4 and plotted in Fig. 6. In this case, both HMM and MsFEM give quite good results in H^1, L^2 and L^∞ norms. This is consistent with the error estimates in Theorems 2.1–2.3.

Table 3
HMM and MsFEM for Problem 3.1 with coefficient (3.2), where $\varepsilon = 1/60$

NX	MsFEM			HMM		
	H^1 error	L^2 error	L^∞ error	H^1 error	L^2 error	L^∞ error
8	0.24e + 0	0.64e − 1	0.84e − 1	0.30e + 0	0.22e − 1	0.23e − 1
16	0.12e + 0	0.24e − 1	0.36e − 1	0.12e + 0	0.78e − 2	0.90e − 2
32	0.67e − 1	0.11e − 1	0.19e − 2	0.63e − 1	0.47e − 2	0.60e − 2
64	0.40e − 1	0.83e − 2	0.15e − 2	0.36e − 1	0.39e − 2	0.52e − 2

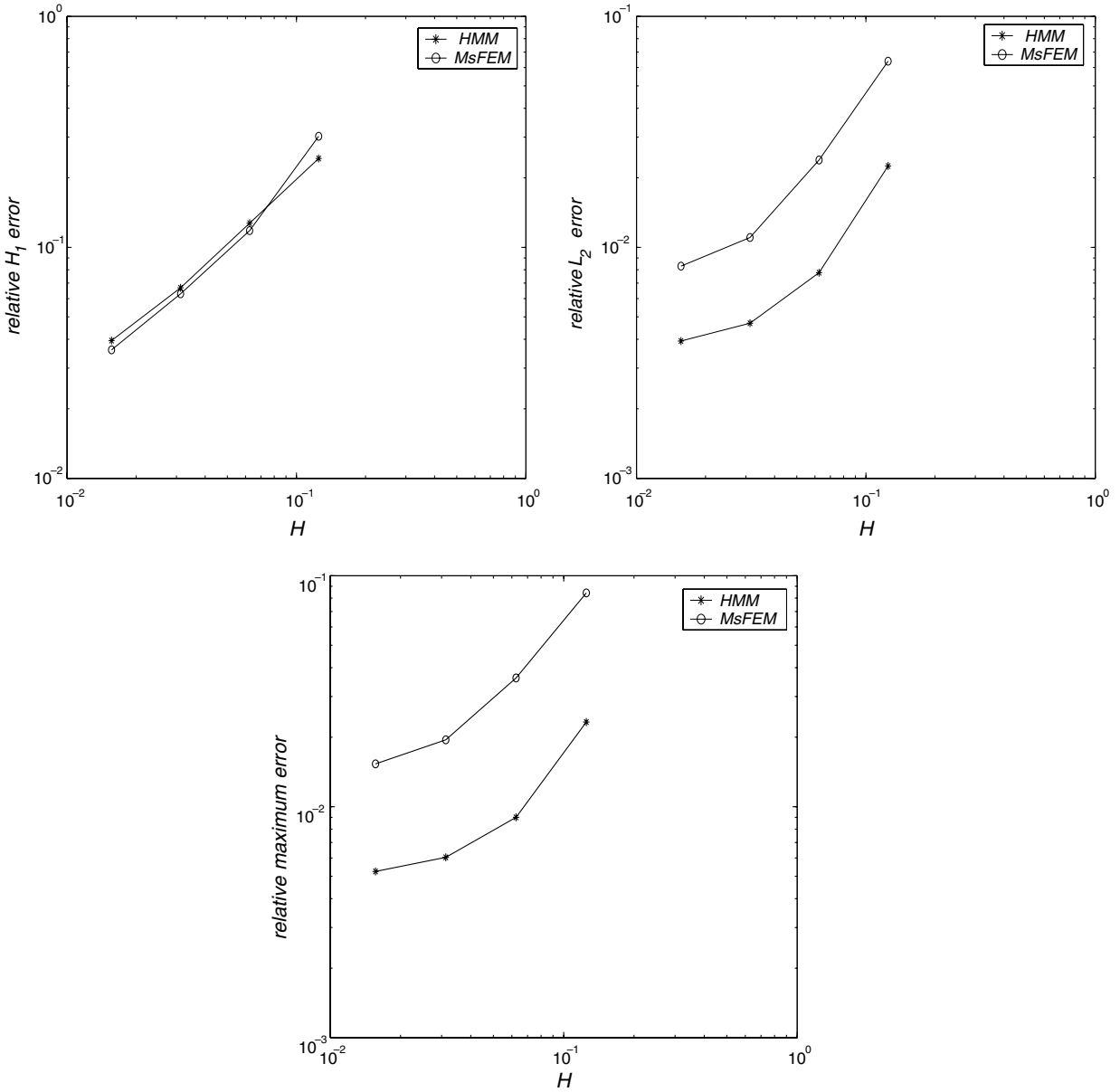

Fig. 5. Relative error in H^1, L^2 and L^∞ norms for HMM and MsFEM for Problem 3.1 with coefficient (3.2), where $\varepsilon = 1/60$ and $I_\delta = I_H$.

Next, we consider the case when the coefficient is random. Some care is required in this case. First of all, to have a well-defined exact solution to the fine scale problem, we will take the fine scale problem to be a finite difference analog of (1.1) on a 1024×1024 grid. The coefficients at the grid points are independent and have

Table 4
HMM and MsFEM for Problem (3.1) with coefficient (3.2), where $\varepsilon = 1/64$. I_ε is used as the microcell of HMM

NX	MsFEM			HMM		
	H^1 error	L^2 error	L^∞ error	H^1 error	L^2 error	L^∞ error
8	0.24e + 00	0.28e − 01	0.32e − 01	0.25e + 00	0.21e − 01	0.22e − 01
16	0.13e + 00	0.13e − 01	0.15e − 01	0.13e + 00	0.79e − 02	0.85e − 02
32	0.69e − 01	0.85e − 02	0.97e − 02	0.64e − 01	0.51e − 02	0.56e − 02
64	0.42e − 01	0.68e − 02	0.78e − 02	0.35e − 01	0.42e − 02	0.46e − 02

log-normal distribution with expectation $\mathbb{E} = \mathbb{0}$ and variance $\sigma^2 = 1$. Therefore, we have $\varepsilon = 1/1024$ [14]. For the HMM solution we choose δ to be H, and $r = H$ for MsFEM solution.

The leading order behavior in this case is determined by the solution of the homogenized equation, which is deterministic. The microscale information comes in at the next order, which is only reflected if one looks at the error in H^1 norm. The results in Fig. 7, which are errors measured in L^2 and L^∞ norms respectively, suggest that both HMM and MsFEM captures the leading order behavior of the solution with reasonable accuracy. MsFEM has better accuracy on very coarse macro-grid. HMM is more accurate upon refining the macroscale mesh. More importantly HMM displays a consistent rate of convergence as the coarse grid is refined.

Next we discuss the issue of extracting the microscale information. This is important for many practical problems such as the stress distribution in a composite material and velocity field in a porous medium. From homogenization theory we know that the microscale information depends sensitively on the full details of the coefficients. Since in HMM the fine scale problem is only solved locally, one cannot hope to recover accurately the details of the fine scale oscillations for each realization of the random field a^ε. Even though MsFEM does make use of the complete information on a^ε and does incur a cost that is at least comparable to that of solving the fine scale problem, the accuracy of MsFEM in H^1 norm (more precisely the piecewise H^1 norm in order to avoid the trouble caused by the discontinuity at the edges between elements), is not much better than 10%. In fact, to recover the fine scale oscillations accurately, one needs to solve the full fine scale problem. Therefore, one should ask instead how the microscale information can be recovered locally, giving the leading order behavior. This is done using the local correction procedure discussed earlier. The results for both HMM and MsFEM are summarized in Tables 5, 6 and Fig. 8. Here, we take K an arbitrarily chosen element and $\eta = 1/8$.

In view of these results, we see consistently that HMM is more accurate than MsFEM on finer macroscale mesh, but less accurate than MsFEM on coarser macroscale mesh. This is likely due to the fact that if the macroscale mesh is very coarse, HMM does not sample a^ε adequately since it only sample a small cell.

3.3. MsFEM does not converge if the fine scale information is not explicitly used

In what follows, we will show by an explicit example that MsFEM does not converge if the small scale information is not explicitly taken into account. Our strategy is similar to *finite difference homogenization* [35,42].

Let $a^\varepsilon(\boldsymbol{x}) = k^\varepsilon(\boldsymbol{x})\mathbf{I}$, where $k^\varepsilon(\boldsymbol{x})$ takes the values α and β as in Fig. 9, ε is the size of the cell, and $\mathbf{I}$ is the 2×2 identity matrix. We may write the coefficient matrix in the form $a^\varepsilon(\boldsymbol{x}) = a(x_1/\varepsilon, x_2/\varepsilon)\mathbf{I}$ with

$$a(y_1, y_2) = \begin{cases} \beta, & 0 \leqslant y_1 \leqslant 1,\ 0 \leqslant y_2 \leqslant y_1, \\ \alpha, & 0 \leqslant y_1 \leqslant 1,\ y_1 \leqslant y_2 \leqslant 1. \end{cases} \tag{3.3}$$

Without using explicitly the information about the size of the microscale, one may take $H = \varepsilon$. We will show in this case that the 'resonance error' remains finite even with oversampling as $H \to 0$. We will take the size of the overlap to be $\delta = rH$ with r fixed.

Lemma 3.1. *Except for the elements near the boundary, the stiffness matrix $A = (A_{ij,k\ell})$ in MsFEM with overlap has the structure*:

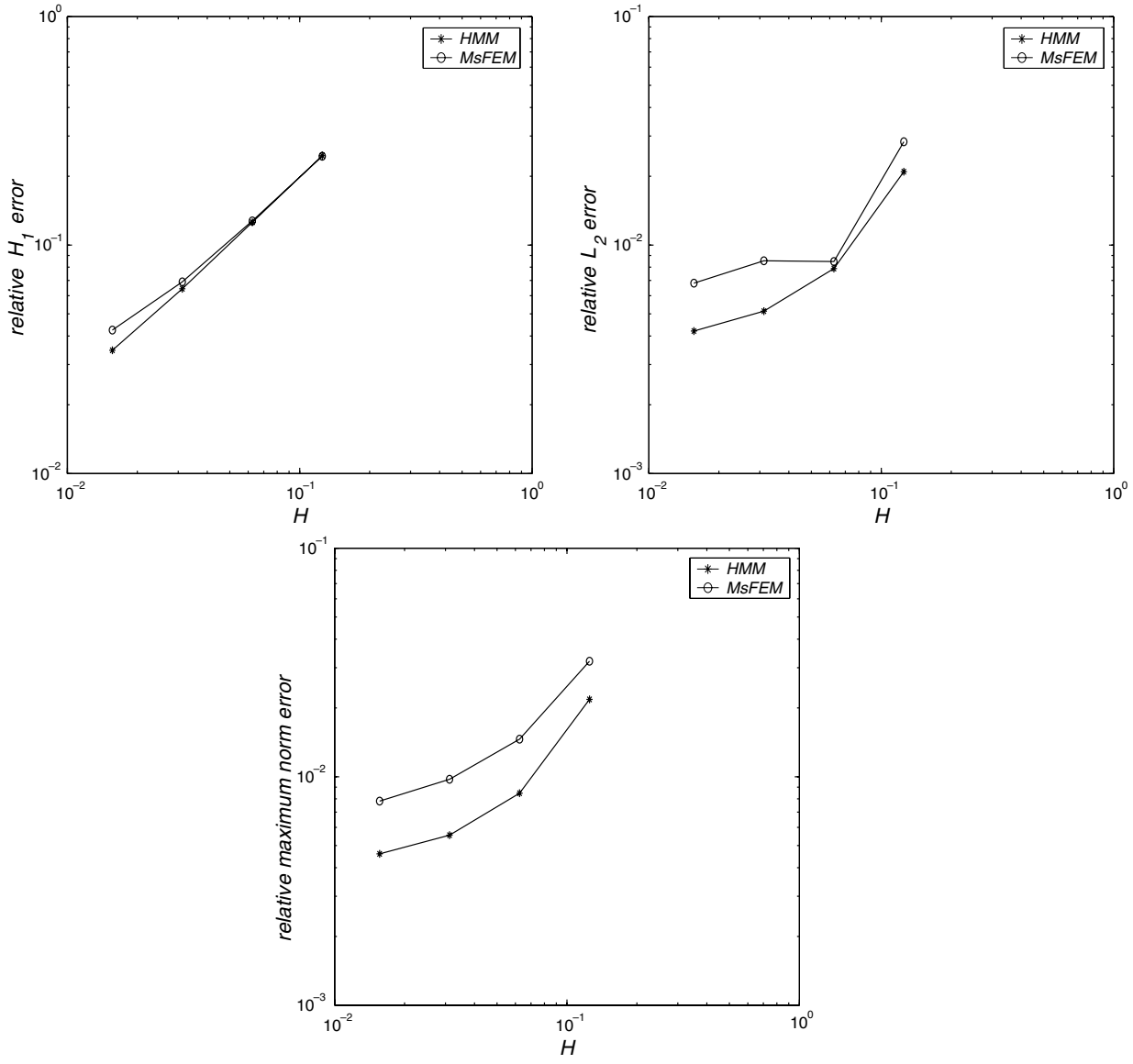

Fig. 6. Relative error in H^1, L^2 and L^∞ norms for HMM and MsFEM for the two scale (3.1) with coefficient (3.2), where $\varepsilon = 1/64$. $I_\delta = I_\varepsilon$.

$$A_{ij;i,j} = b, \quad A_{ij;i-1,j} = c, \quad A_{ij;i,j-1} = c,$$
$$A_{ij;i+1,j} = c, \quad A_{ij;i,j+1} = c,$$
$$A_{ij;i-1,j+1} = d, \quad A_{ij;i+1,j-1} = d,$$

where b, c and d depend on r but are independent of H. Moreover,

$$b + 4c + 2d = 0. \tag{3.4}$$

Proof. This follows from the simple observation that after some reflection and translation if necessary, every element can be mapped by a simple scaling $(x,y) \to (x/H, y/H)$ to the standard element shown in Fig. 10. We postpone the proof of (3.4) to Appendix A. □

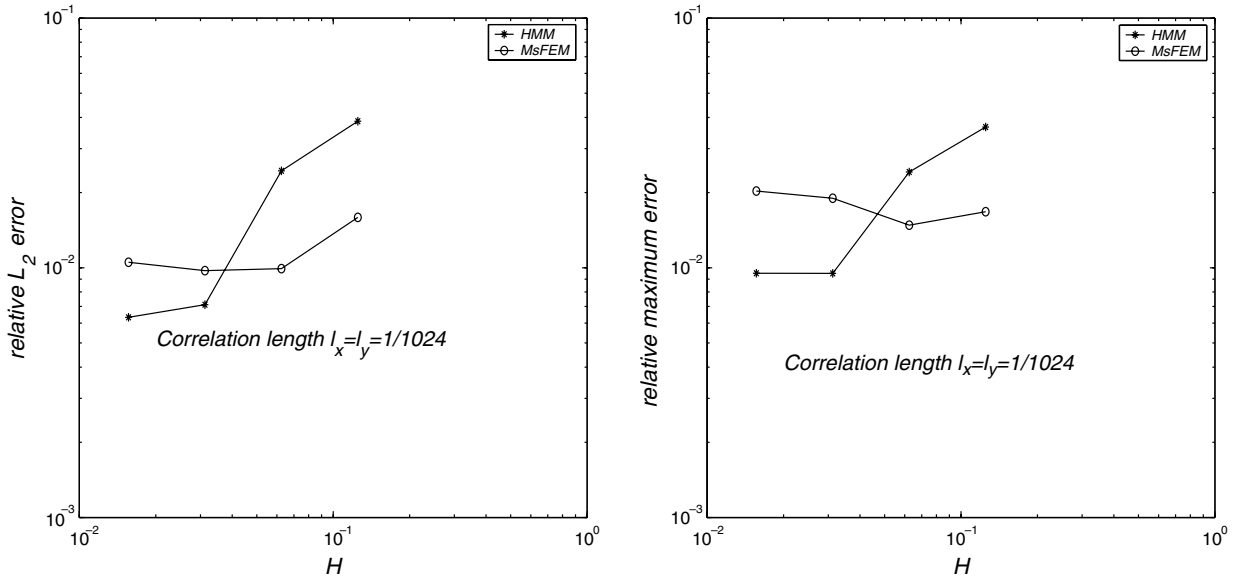

Fig. 7. Relative error in L^2 and L^∞ norms for Problem 3.1 with random coefficients.

Table 5
MsFEM for Problem 3.1 with random coefficients, H^1 error (1) means the results are obtained with correction, and H^1 error (2) means the results are obtained without correction

NX	MsFEM			
	H^1 error(1)	H^1 error(2)	L^2 error	L^∞ error
8	0.28e − 1	0.22e + 0	0.16e − 1	0.17e − 1
16	0.11e − 1	0.12e + 0	0.99e − 2	0.15e − 1
32	0.86e − 2	0.81e − 1	0.97e − 2	0.19e − 1
64	0.88e − 2	0.99e − 1	0.11e − 1	0.20e − 1

Table 6
HMM for Problem 3.1 with random coefficients, H^1 error (1) means the results are obtained with correction, and H^1 error (2) means the results are obtained without correction

NX	HMM			
	H^1 error(1)	H^1 error(2)	L^2 error	L^∞ error
8	0.34e − 1	0.27	0.39e − 1	0.37e − 1
16	0.19e − 1	0.23	0.24e − 1	0.24e − 1
32	0.48e − 2	0.21	0.71e − 2	0.95e − 2
64	0.41e − 2	0.26	0.63e − 2	0.95e − 2

Lemma 3.2. *As $H \to 0$, the solution of MsFEM converges to the solution of*

$$-e(r)\triangle U_0(\boldsymbol{x}) - 2f(r)\partial_{xy}U_0(\boldsymbol{x}) = f(\boldsymbol{x}), \tag{3.5}$$

where $e(r) = -c-d$ and $f(r) = d$.

Proof. This follows directly from Lemma 3.1 by Taylor expansion. □

Lemma 3.3. *In the special case when $r = 0$ (no overlapping), then*

$$b = 2(\alpha+\beta), \qquad c = -\frac{\alpha+\beta}{2}, \qquad d = 0.$$

Proof. This is straightforward. □

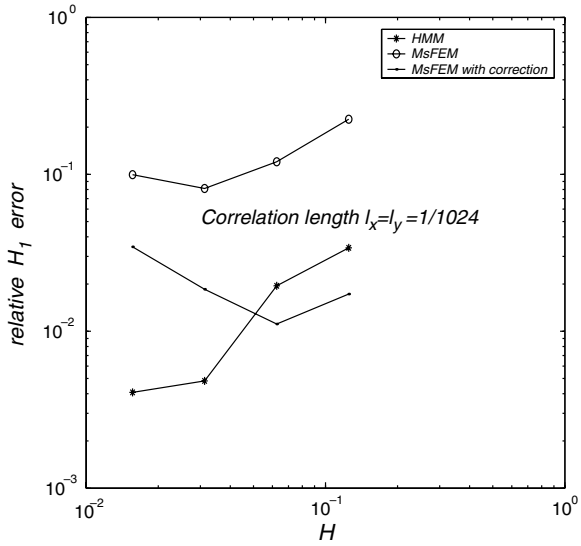

Fig. 8. Relative error in H^1 norm for Problem 3.1 with random coefficients.

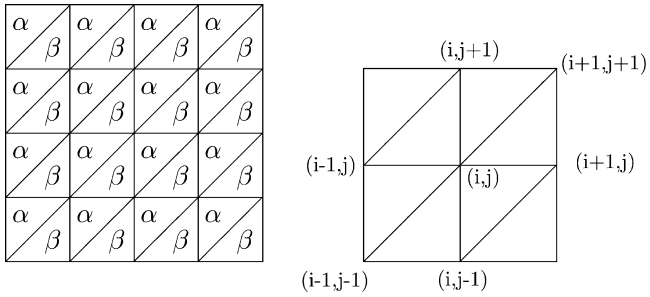

Fig. 9. Left, pattern for $\varepsilon = H$. Right: element stiffness matrix.

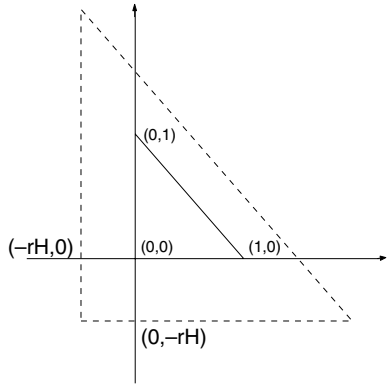

Fig. 10. Pattern for $\varepsilon = H$ with overlap r.

As $\varepsilon = H \to 0$, the original problem, however, is a homogenization problem [7,46], whose homogenized coefficient has the following property.

Lemma 3.4. *The homogenized coefficient matrix A has the following structure*

$$A = \begin{pmatrix} e^* & f^* \\ f^* & e^* \end{pmatrix},$$

where e^* and f^* satisfy the following relation

$$(e^*)^2 - (f^*)^2 = \alpha\beta. \tag{3.6}$$

To prove the above lemma, we first give a description for the properties of the homogenized coefficient matrix for the elliptic problem (1.1), which is denoted by A and is given by

$$A_{ij} = \int_0^1 \int_0^1 \left(a_{kl} \frac{\partial \chi^i}{\partial x_k} \frac{\partial \chi^j}{\partial x_l} \right)(\boldsymbol{x})\, \mathrm{d}\boldsymbol{x}, \quad i,j = 1,2,$$

where $\chi^j = x_j + N^j$, and N^j is periodic function that satisfies

$$-\frac{\partial}{\partial x_i}\left(a_{ik} \frac{\partial N^j}{\partial x_k} \right) = \frac{\partial a_{ij}}{\partial x_i}, \quad j = 1,2. \tag{3.7}$$

Since a^ε is diagonal, we get

$$A_{ij} = \int_0^1 \int_0^1 (a^\varepsilon \nabla \chi^i \nabla \chi^j)(\boldsymbol{x})\, \mathrm{d}\boldsymbol{x}. \tag{3.8}$$

Denote by $\bar{a}^\varepsilon$ and $\hat{a}^\varepsilon$ the coefficients obtained by reflecting the pattern in Fig. 9 along the x_1 and x_2 axis, respectively (see Fig. 11 below), $\bar{A}$ and $\hat{A}$ denote the corresponding effective coefficient matrix.

Lemma 3.5. *If*

$$A = \begin{pmatrix} a & b \\ b & c \end{pmatrix},$$

then we have

$$\bar{A} = \begin{pmatrix} a & -b \\ -b & c \end{pmatrix}, \quad \hat{A} = \begin{pmatrix} a & b \\ b & c \end{pmatrix}.$$

Proof. Denote by $\bar{N}^j$ the solutions of the cell problem (3.7) with coefficients $\bar{a}^\varepsilon$, then

$$\bar{N}^1(x,y) = N^1(x,1-y), \quad \bar{N}^2(x,y) = -N^2(x,1-y). \tag{3.9}$$

In view of (3.8), we get the above expression for $\bar{A}$. Proceeding in the same fashion, we get the above expression for $\hat{A}$. □

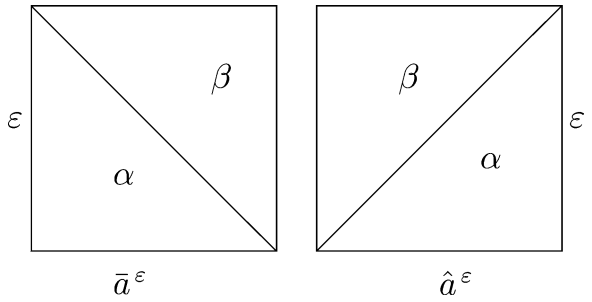

Fig. 11. The pattern for the coefficients $\bar{a}^\varepsilon$ and $\hat{a}^\varepsilon$.

Proof for Lemma 3.4. Observe that A is symmetric since a^ε is symmetric, we thus assume

$$A = \begin{pmatrix} e^* & f^* \\ f^* & \tilde{e}^* \end{pmatrix}.$$

Since $\bar{a}^\varepsilon$ is symmetric with respect to the line $x = y$, we may conclude that

$$\bar{N}^1(x,y) = \bar{N}^2(y,x),$$

which implies $e^* = \tilde{e}^*$. Invoking Lemma 3.5, we have $A = \hat{A}$. Using the general duality principle in homogenization theory [47, Theorem 15.1] (see also [34]), we have

$$\mathscr{R} A \mathscr{R}^T \hat{A} = \mathrm{diag}(\alpha\beta, \alpha\beta),$$

where $\mathscr{R}$ is the rotation matrix with angle $\pi/2$ and $\mathscr{R}^T$ is the transpose matrix, i.e.,

$$\mathscr{R} = \begin{pmatrix} 0 & 1 \\ -1 & 0 \end{pmatrix}.$$

From this we obtain $(e^*)^2 - (f^*)^2 = \alpha\beta$. □

We can check by direct computation whether (3.6) is satisfied by the solutions of MsFEM. When $r = 0$, we have $e(0) = \frac{\alpha+\beta}{2}$ and $f(0) = 0$, hence

$$e(0)^2 - f(0)^2 = \left(\frac{\alpha+\beta}{2}\right)^2 \neq \alpha\beta.$$

In Fig. 12, we plot $e^*(r)^2 - f^*(r)^2$ as a function of r in case of $\alpha = 10$ and $\beta = 1$ hence $\alpha\beta = 10$. We can see that when $r > 0$, the error $e^*(r)^2 - f^*(r)^2 - \alpha\beta$ is reduced but stays finite, proving that there is a finite error in the solutions of MsFEM when $H \to 0$.

These findings are consistent with the error estimates in Theorem 2.3 suggesting that the term ε/H does play a role in the error.

To recover convergence to the correct solution within the framework of MsFEM, we need to take $H \gg \varepsilon$. However in this case as we indicated earlier, either MsFEM has to be modified to tailor to the specific periodic structure, or efficiency has to be greatly compromised.

Remark 3.6. This example is also applicable to HMM. However, as we stated in the very first that HMM does not work for problems without scale separation.

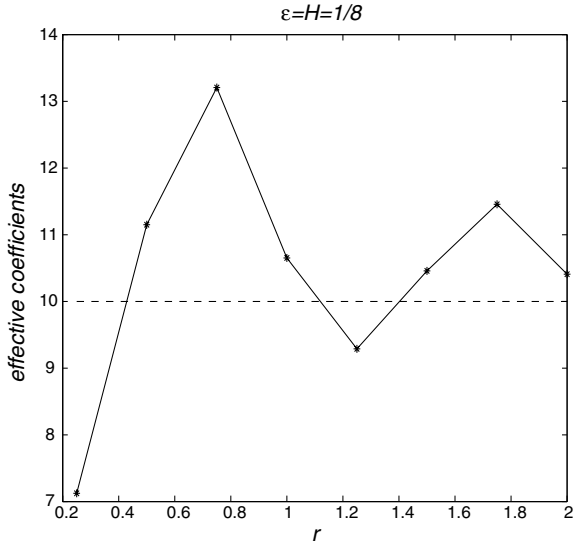

Fig. 12. Comparison of $e^*(r)^2 - f^*(r)^2$ computed by MsFEM (the solid line) and the exact value of $(e^*)^2 - (f^*)^2 = 10$ (the dashed line).

4. Problems without scale separation

4.1. Problems with many scales

It has been observed that for some problems without scale separation, MsFEM does seem to give answers with reasonable accuracy. We have experimented with a number of such examples. We found that this is not special to MsFEM. HMM also shows the same tendency. In this case since there is no scale separation, we choose size of the cell I_δ to be the same as H. Hence there is no savings compared with the fine scale solver.

We show the result of one example with six scales. We solve (2.1) with the following coefficients.

$$a^\varepsilon(\boldsymbol{x}) = \frac{1}{6}\left(\frac{1.1+\sin(2\pi x/\varepsilon_1)}{1.1+\sin(2\pi y/\varepsilon_1)} + \frac{1.1+\sin(2\pi y/\varepsilon_2)}{1.1+\cos(2\pi x/\varepsilon_2)} + \frac{1.1+\cos(2\pi x/\varepsilon_3)}{1.1+\sin(2\pi y/\varepsilon_3)} + \frac{1.1+\sin(2\pi y/\varepsilon_4)}{1.1+\cos(2\pi x/\varepsilon_4)} + \frac{1.1+\cos(2\pi x/\varepsilon_5)}{1.1+\sin(2\pi y/\varepsilon_5)} + \sin(4x^2y^2) + 1\right), \tag{4.1}$$

where $\varepsilon_1 = 1/5$, $\varepsilon_2 = 1/13$, $\varepsilon_3 = 1/17$, $\varepsilon_4 = 1/31$ and $\varepsilon_5 = 1/65$. The right-hand side is $f = 10$. The coefficient at $y = 0$ is plotted in Fig. 13.

The results for the relative error in H^1, L^2 and L^∞ norms are plotted in Fig. 14. As before the exact solution is obtained by extrapolating the numerical solutions on the 1024×1024 and 2048×2048 meshes. We can see from these results that the accuracy is substantially worse than the case with scale separation, but it is not catastrophic and maybe acceptable for some practical problems.

Even though the accuracy seems to be reasonable, one has to bear in mind two facts. The first is that in this case the cost of either HMM or MsFEM is no less than that of the fine scale solver. The second is that the accuracy is substantially less than that of the fine scale solver. In fact the example discussed earlier in subsection 3.3 shows that in general one has to expect a finite error to remain in the limit as $H \to 0$. These considerations remove any interest of pursuing the issue further.

Compared with the two-scale problems addressed before, the above convergence history for both methods indicates quite pessimistic convergence rate, in particular for the results in H^1 norm. The oscillation is also significant in both methods, which might be the result of the resonance error between different scales.

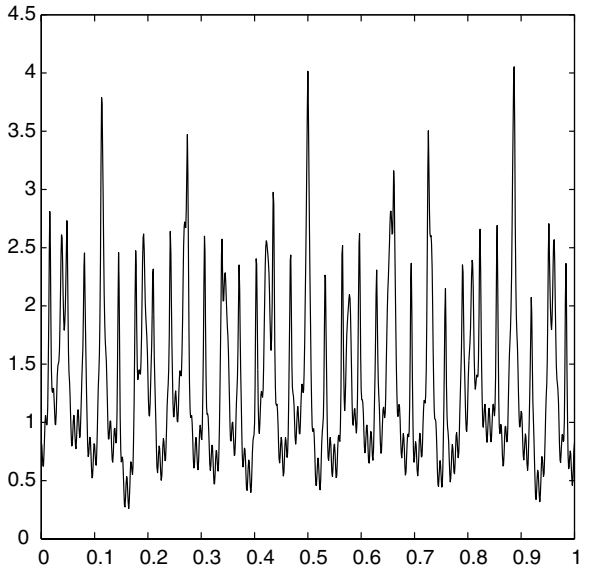

Fig. 13. The coefficient (4.1) at $y = 0$.

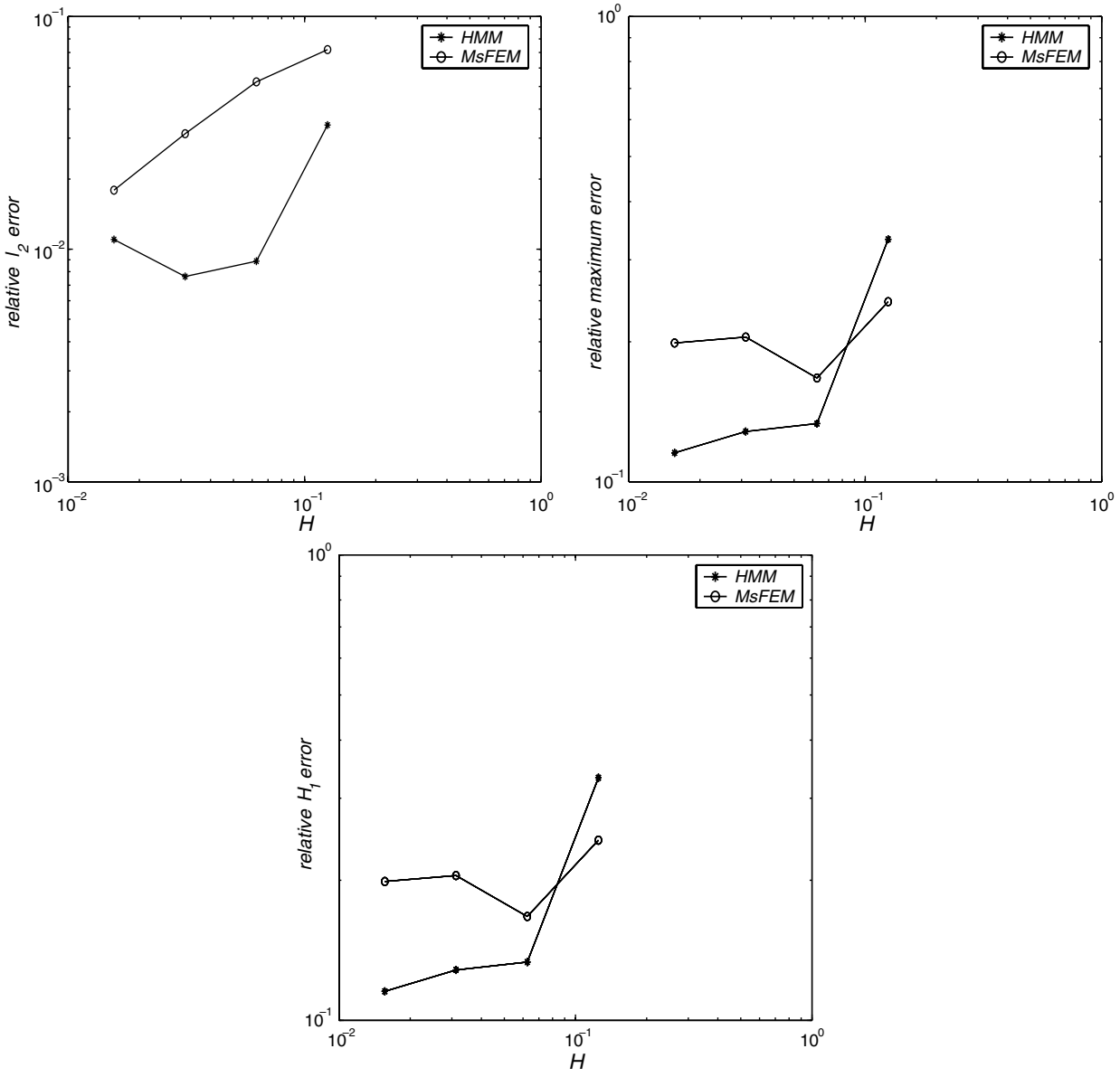

Fig. 14. Relative error for HMM and MsFEM in H^1, L^2 and $L^\infty-$norms for the problem (3.1) with coefficient (4.1).

4.2. Problems with continuous spectrum

Another often used example of problems without scale separation is the problem with random coefficients that have an algebraically decaying energy spectrum, i.e.,

$$\langle|\hat{a}(k)|^2\rangle \simeq |,k|^{-\alpha},$$

where $\langle\cdot\rangle$ denotes ensemble averaging, $\{\hat{a}(k)\}$ is the Fourier transform of the coefficients $a(x)$. Problems of this kind were used in [31] as examples without scale separation. We will demonstrate in this case that u has some degree of regularity depending on α, hence standard finite element methods converge with certain rate. Even though there is no scale separation in this problems, the energy content decreases as the scale decreases. Hence there is relatively little energy at this small scale. This gives rise to the regularity of the solutions. Therefore,

this class of problems are in fact much simpler than the one considered earlier in which the small scale and the large scale have the comparable amount of energy.

We consider the following problem:

$$\begin{cases} -\frac{\mathrm{d}}{\mathrm{d}x}\left(a(x)\frac{\mathrm{d}u}{\mathrm{d}x}\right) = \frac{\mathrm{d}}{\mathrm{d}x}g(x) & \text{in } [0,1], \\ u(x) = 0 & x = 0, 1. \end{cases} \tag{4.2}$$

Here

$$a(x) = 1 + \frac{1}{2}\sin\left(\sum_{k=1}^{\infty} k^{-\alpha}(\xi_{1k}\sin(kx) + \xi_{2k}\cos(kx))\right) \tag{4.3}$$

with $\{\xi_{1k}\}$ and $\{\xi_{2k}\}$ are two independent random sequences uniformly distributed in $[-1/2, 1/2]$.

This problem by itself is specific, but our discussions are quite general. The regularity of $a(x)$ depends on the regularity of

$$g(x) = \sum_{k=1}^{\infty} k^{-\alpha}(\xi_{1k}\sin(kx) + \xi_{2k}\cos(kx)). \tag{4.4}$$

In particular for $\beta > 0$

$$\langle \|g(x)\|_{H^\beta}^2 \rangle \leqslant C\sum_{k=1}^{\infty} k^{2(\beta-\alpha)} < \infty,$$

if $\beta < \alpha - \frac{1}{2}$.

The exact solution satisfies

$$u_x(x) = \frac{g(x)}{1 + \frac{1}{2}\sin(g(x))}.$$

Hence we expect

$$\langle \|u(x)\|_{H^{1+\beta}} \rangle < \infty \qquad \text{if} \quad \beta < \alpha - 1/2.$$

Consequently, the standard linear finite element method with mesh size h should have the estimate:

$$\langle \|u(x) - u_h(x)\|_{H^1} \rangle \leqslant Ch^\beta, \tag{4.5}$$

for β arbitrarily close to $\alpha - 1/2$, if $0 < \alpha - 1/2 < 1$.

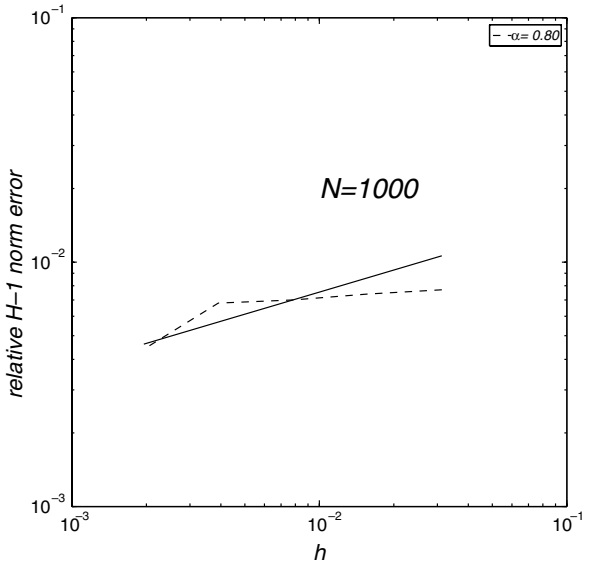

Fig. 15. Relative H^1 error for $\alpha = 0.80$. The solid line is the reference curve for $h^{\alpha-1/2}$.

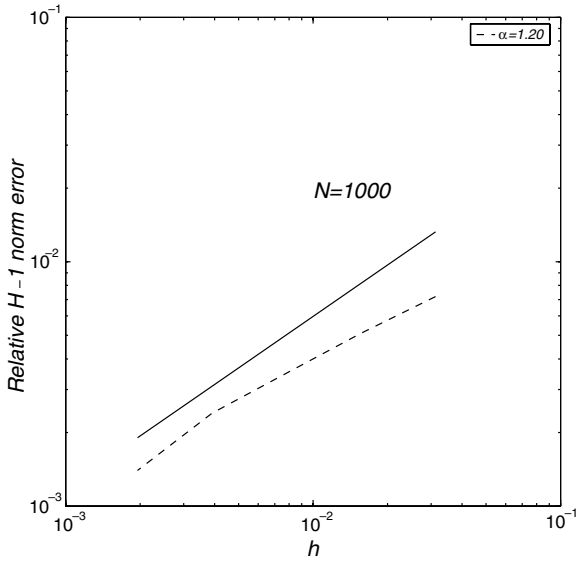

Fig. 16. Relative H^1 error for $\alpha = 1.20$. The solid line is the reference curve for $h^{\alpha-1/2}$.

We performed numerical experiments on this problem. Plotted in Figs. 15 and 16 are the convergence history of the standard piecewise linear finite element method for one realization of (4.3) and (4.4) with $\alpha = 0.8$ and 1.2, respectively. We see that (4.5) is confirmed quite well.

To make a direct comparison between the different methods for this case would require tuning too many parameters. However this result and that of [31] do suggest that at the same cost the direct fine scale solver will perform at least as well as MsFEM, because of the regularity of the exact solution. The same is expected for HMM.

5. Conclusions

We have reviewed a variety of numerical techniques for solving the elliptic problem with multiscale coefficients. These techniques can be divided into two categories, those that are specifically designed for periodic homogenization problems and those that are applicable for more general problems. The former includes methods that solve the homogenized and corrector equations, finite elements methods that use multiscale test and trial functions. The latter includes HMM and MsFEM.

An important issue is how the cost of these methods compares with techniques such as multigrid for solving the full fine scale problem. In particular, whether some special features of the problems, such as scale separation, can be exploited to save cost. Nearly all the methods reviewed do have such savings for the special problem of periodic homogenization. For more general problems, the framework of HMM still allows us to take full advantage of any scale separation in the problem and therefore reduces the cost. This is different from MsFEM, which in general incurs a cost that is comparable to that of solving the full fine scale problem.

Many problems in practice do not have scale separation. Care has to be exercised when treating these problems. In the absence of any other special features of the problem, there is no hope to design numerical methods with sublinear cost compared with the fine scale solver. Therefore the task becomes identifying classes of problems with some other special features that can be made use of in order to reduce cost.

Acknowledgements

We thank Professor Weinan E and Professor Bjorn Engquist for inspiring discussions on the topic studied here. The work of Ming is partially supported by National Natural Science Foundation of China under the grant 10571172 and the National Basic Research Program under the grant 2005CB321704. The work of Yue is

supported in part by NSF of China under the grant 10471102 and in part by the national basic research program under the grant 2005CB321704.

Appendix A. Proof of (3.4)

There are only two types of triangles in the pattern of Fig. 9, i.e., we associate ϕ_i and ψ_i the MsFEM bases of ith vertices in triangles K_1 and K_2, respectively. Define

$$\langle \phi_i, \phi_j \rangle = \int_{K_1} \nabla \phi_i \nabla \phi_j \, d\boldsymbol{x}, \quad \langle \psi_i, \psi_j \rangle = \int_{K_2} \nabla \psi_i \nabla \psi_j \, d\boldsymbol{x}.$$

Proof of 3.4. For ease of exposition, we drop the first subscript index of A. We first derive the following explicit expression for b,c and d (See Fig. A.1).

$$b = 2\beta\langle \phi_2, \phi_2 \rangle + 2\alpha\langle \psi_3, \psi_3 \rangle - 2\beta\langle \phi_1, \phi_3 \rangle - 2\alpha\langle \psi_1, \psi_2 \rangle$$

and

$$c = -\frac{\beta}{2}\langle \phi_2, \phi_2 \rangle - \frac{\alpha}{2}\langle \psi_3, \psi_3 \rangle,$$
$$d = \beta\langle \phi_1, \phi_3 \rangle + \alpha\langle \psi_1, \psi_2 \rangle.$$

Due to the symmetry, we only consider a typical cell. Observed that

$$\sum_{i=1}^{3} \phi_i = 1, \quad \sum_{i=1}^{3} \psi_i = 1,$$

with

$$\phi_1(x_1, x_2) = \phi_3(-x_2, -x_1), \quad \psi_1(x_1, x_2) = \psi_2(-x_2, -x_1). \tag{A.1}$$

Obviously,

$$b = \beta \sum_{i=1}^{3} \langle \phi_i, \phi_i \rangle + \alpha \sum_{i=1}^{3} \langle \psi_i, \psi_i \rangle.$$

In view of the first observation, we get

$$\begin{aligned} \langle \phi_1, \phi_1 \rangle + \langle \phi_3, \phi_3 \rangle - \langle \phi_2, \phi_2 \rangle + 2\langle \phi_2, \phi_2 \rangle &= \langle \phi_1, \phi_1 \rangle + \langle \phi_3, \phi_3 \rangle - \langle \phi_1 + \phi_3, \phi_1 + \phi_3 \rangle + 2\langle \phi_2, \phi_2 \rangle \\ &= -2\langle \phi_1, \phi_3 \rangle + 2\langle \phi_2, \phi_2 \rangle. \end{aligned}$$

Similarly

$$\sum_{i=1}^{3} \langle \psi_i, \psi_i \rangle = -2\langle \psi_1, \psi_2 \rangle + 2\langle \psi_3, \psi_3 \rangle.$$

A combination of the above two leads to the expression for b.

It remains to prove the expression for c. We have $A_{i,j+1} = \beta\langle \phi_2, \phi_3 \rangle + \alpha\langle \psi_1, \psi_3 \rangle$ and $A_{i+1,j} = \beta\langle \phi_1, \phi_2 \rangle + \alpha\langle \psi_2, \psi_3 \rangle$. Due to observation (A.1), we get

$$\langle \phi_2, \phi_1 - \phi_3 \rangle = -\langle \phi_1 + \phi_3, \phi_1 - \phi_3 \rangle = \langle \phi_3, \phi_3 \rangle - \langle \phi_1, \phi_1 \rangle = 0.$$

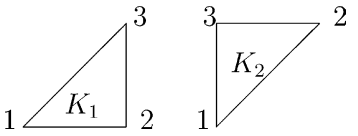

Fig. A.1.

Similarly, $\langle\psi_1,\psi_3\rangle = \langle\psi_2,\phi_3\rangle$. We thus have $A_{i,j+1} = A_{i+1,j}$, then

$$2A_{i,j+1} = A_{i,j+1} + A_{i+1,j} = -\beta\langle\phi_2,\phi_2\rangle - \alpha\langle\psi_3,\psi_3\rangle.$$

It follows the expression for c. The expression for d is obtained by the definition. With these expressions, it follows (3.4). □

References

[1] R.A. Adams, Sobolev Spaces, Academic Press, 1975.
[2] R.E. Alcouffe, A. Brandt, J.E. Dendy, J.W. Painter, The multigrid method for the diffusion equation with strongly discontinuous coefficients, SIAM J. Sci. Statist. Comput. 2 (1981) 430–454.
[3] G. Allaire, Homogenization and two-scale convergence, SIAM J. Math. Anal. 23 (1992) 1482–1518.
[4] I. Babuska, Homogenization and its applications, mathematical and computational problems, in: B. Hubbard (Ed.), Numerical Solutions of Partial Differential Equations-III, (SYNSPADE 1975, College Park MD, May 1975), Academic Press, New York, 1976, pp. 89–116.
[5] I. Babuska, Solution of interface problems by homogenization I, II, III, SIAM J. Math. Anal. 7 (1976) 603–634, pp. 635–645; I. Babuska, Solution of interface problems by homogenization I, II, III, SIAM J. Math. Anal. 8 (1977) 923–937.
[6] I. Babuska, G. Caloz, J. Osborn, Special finite element methods for a class of second order elliptic problems with rough coefficients, SIAM J. Numer. Anal. 31 (1994) 945–981.
[7] I. Babuska, J. Osborn, Generalized finite element methods: their performance and their relation to mixed methods, SIAM J. Numer. Anal. 20 (1983) 510–536.
[8] A. Bensoussan, J.L. Lions, G.C. Papanicolaou, Boundary layer analysis in homogenization of diffusion equations with Dirichlet cnditions on the half spaces, in: K. Ito (Ed.), Proceedings of International Symposium on Stochastic Differential Equations, Wiley, New York, 1976, pp. 21–40.
[9] A. Bensoussan, J.L. Lions, G.C. Papanicolaou, Asymptotic Analysis for Periodic Structures, North-Holland, Amsterdam, 1978.
[10] J.F. Bourgat, Numerical experiments of the homogenization method for operators with periodic coefficients, Lecture Notes in Mathematics, vol. 707, 1977, pp. 330–356.
[11] A. Brandt, Multi-level adaptive solutions to boundary-value problems, Math. Comp. 31 (1977) 333–390.
[12] F. Brezzi, L.P. Franca, T.J.R. Hughes, A. Russo, $b = \int g dx$, Comput. Meth. Appl. Mech. Eng. 145 (1997) 329–339.
[13] Z. Chen, T. Hou, A mixed multiscale finite element method for elliptic problems with oscillating coefficients, Math. Comp. 72 (2003) 541–576.
[14] J.G. Conlon, A. Naddaf, On homogenization of elliptic equations with random coefficients, Electron J. Probab. 5 (2000) 1–58.
[15] J.Z. Cui, L.Q. Chao, The two-scale analysis methods for woven composite materials, in: Zhi-hua Zhong (Ed.), Engineering Computation and Computer Simulation I, Hunan University Press, 1995, pp. 203–212.
[16] L.J. Durlofsky, Numerical-calculation of equivalent grid block permeability tensors for heterogenous porous media, Water Resour. Res. 27 (1991) 699–708.
[17] M. Dorobantu, B. Engquist, Wavelet-based numerical homogenization, SIAM J. Numer. Anal. 35 (1998) 540–559.
[18] W. E, Homogenization of linear and nonlinear transport equations, Comm. Pure Appl. Math. 45 (1992) 301–326.
[19] W. E, B. Engquist, The heterogeneous multiscale methods, Commun. Math. Sci. 1 (2003) 87–132.
[20] W. E, B. Engquist, The heterogeneous multiscale method for homogenization problems, MMS (submitted).
[21] W. E, B. Engquist, Multiscale modeling and computation, Notice Amer. Math. Soc. 50 (2003) 1062–1070.
[22] W. E, P. Ming, P. Zhang, Analysis of the heterogeneous multiscale method for elliptic homogenization problems, J. Am. Math. Soc. 18 (2005) 121–156.
[23] Y.R. Efendiev, T. Hou, V. Ginting, Multiscale finite element methods for nonlinear problems and their applications, Commun. Math. Sci. 2 (2004) 553–589.
[24] Y.R. Efendiev, T. Hou, X. Wu, Convergence of a nonconforming multiscale finite element method, SIAM J. Numer. Anal. 37 (2000) 888–910.
[25] B. Engquist, O. Runborg, Wavelet-based numerical homogenization with applications, in: T.J. Barth, T. Chan, R. Heimes (Eds.), Multiscale and Multiresolution Methods: Theory and Applications, Lecture Notes in Computational Sciences and Engineering, vol. 20, Springer-Verlag, Berlin, 2002, pp. 97–148.
[26] C. Farhat, I. Harari, L.P. Franca, The discontinuous enrichment method, Comput. Meth. Appl. Mech. Eng. 190 (2001) 6455–6479.
[27] J. Fish, V. Belsky, Multigrid method for a periodic heterogeneous medium, Part I: Convergence studies for one-dimensional case, Comput. Meth. Appl. Mech. Eng. 126 (1995) 1–16.
[28] J. Fish, V. Belsky, Multigrid method for a periodic heterogeneous medium, Part I: Multiscale modeling and quality in multi-dimensional case, Comput. Meth. Appl. Mech. Eng. 126 (1995) 17–38.
[29] J. Fish, Z. Yuan, Multiscale enrichment based on partition of unity, Inter. J. Numer. Meth. Eng. 62 (2005) 1341–1359.
[30] L. Greengard, V. Rokhlin, A fast algorithm for particle simulations, J. Comput. Phys. 73 (1987) 325–348.
[31] T. Hou, X. Wu, A multiscale finite element method for elliptic problems in composite materials and porous media, J. Comput. Phys. 134 (1997) 169–189.
[32] T. Hou, X. Wu, Z. Cai, Convergence of a multiscale finite element method for elliptic problems with rapidly oscillating coefficients, Math. Comp. 68 (1999) 913–943.

[33] T.J.R. Hughes, Multiscale phenomena: Green's functions, the Dirichlet to Neumann formulation, subgrid scale models, bubbles and the origin of stabilized methods, Comput. Meth. Appl. Mech. Eng. 127 (1995) 387–401.
[34] J.B. Keller, A theorem on the conductivity of a composite medium, J. Math Phys. 5 (1964) 548–549.
[35] S.M. Kozlov, Averaging of difference schemes, Math. USSR Sbornik. 57 (1987) 351–369.
[36] A.M. Matache, I. Babuska, C. Schwab, Generalized p-FEM in homogenization, Numer. Math. 86 (2000) 319–375.
[37] A.M. Matache, C. Schwab, Two-scale finite element for homogenization problems, M2AN Math. Model. Numer. Anal. 36 (2002) 537–572.
[38] J.D. Moulton, J.E. Dendy, J.M. Hyman, The black box multigrid numerical homogenization algorithm, J. Comput. Phys. 141 (1998) 1–29.
[39] N. Neuss, W. Jäger, G. Wittum, Homoginization and multigrid, Computing 66 (2001) 1–26.
[40] G. Nguetseng, A general convergence result for a functional related to the theory of homogenization, SIAM J. Math. Anal. 20 (1989) 608–623.
[41] J.T. Oden, K.S. Vemaganti, Estimation of local modeling error and global-oriented adaptive modeling of heterogeneous materials. I: Error estimates and adaptive algorithms, J. Comput. Phys. 164 (2000) 22–47.
[42] A. Piatnitski, E. Remy, Homogenization of elliptic difference operators, SIAM J. Math. Anal. 33 (2001) 53–83.
[43] G. Sangalli, Capturing small scales in elliptic problems using a Residual-Free Bubbles finite element method, Multiscale Model. Simul. 1 (2003) 485–503.
[44] C. Schwab, Two-scale FEM for homogenization problems, in: I. Babuska, P.G. Ciarlet, T. Miyoshi (Eds.), Mathematical Modeling and Numerical Simulation in Continuum Mechanics, Lecture Notes in Computational Science and Engineering, vol. 19, Springer-Verlag, Berlin, 2002, pp. 91–108.
[45] C. Schwab, A.M. Matache, Generalzied FEM for homogenization problems, in: T.J. Barth, T. Chan, R. Heimes (Eds.), Multiscale and Multiresolution Methods: Theory and Applications, Lecture Notes in Computational Sciences and Engineering, vol. 20, Springer-Verlag, Berlin, 2002, pp. 197–238.
[46] L. Tartar, Estimations de coefficients homogénéisésLecture notes in Mathematics, vol. 704, Springer-Verlag, Berlin, 1979, pp. 364–373.
[47] S. Torquato, Random Heterogeneous Materials: Microstructure and Macroscopic Properties, Springer-Verlag, New York, 2002.
[48] X.Y. Yue, Numerical homogenization for well-driven transport in heterogeneus media, Report, Institute of Computational Mathematics, AMSS, Chinese Academy of Sciences, 2002.
[49] V.V. Zhikov, S.M. Kozlov, O.A. Oleinik, Homogenization of Differential Operators and Integral Functionals, Springer-Verlag, Heidelberg, 1994.